



Fourier decomposition of polymer orientation in large-amplitude oscillatory shear flow

A. J. Giacomin, P. H. Gilbert, and A. M. Schmalzer

Citation: *Structural Dynamics* **2**, 024101 (2015); doi: 10.1063/1.4914411

View online: <http://dx.doi.org/10.1063/1.4914411>

View Table of Contents: <http://scitation.aip.org/content/aca/journal/sdy/2/2?ver=pdfcov>

Published by the American Crystallographic Association, Inc.

Articles you may be interested in

[Layering, melting, and recrystallization of a close-packed micellar crystal under steady and large-amplitude oscillatory shear flows](#)

J. Rheol. **59**, 793 (2015); 10.1122/1.4917542

[Dilute rigid dumbbell suspensions in large-amplitude oscillatory shear flow: Shear stress response](#)

J. Chem. Phys. **140**, 074904 (2014); 10.1063/1.4862899

[Nonlinear viscoelasticity of polymer nanocomposites under large amplitude oscillatory shear flow](#)

J. Rheol. **57**, 767 (2013); 10.1122/1.4795748

[Viscous heating in large-amplitude oscillatory shear flow](#)

Phys. Fluids **24**, 103101 (2012); 10.1063/1.4752777

[Yielding processes in a colloidal glass of soft star-like micelles under large amplitude oscillatory shear \(LAOS\)](#)

J. Rheol. **54**, 1219 (2010); 10.1122/1.3483610

Fourier decomposition of polymer orientation in large-amplitude oscillatory shear flow

A. J. Giacomin,^{1,2,a)} P. H. Gilbert,¹ and A. M. Schmalzer³

¹*Chemical Engineering Department, Polymers Research Group, Queen's University, Kingston, Ontario K7L 3N6, Canada*

²*Mechanical and Materials Engineering Department, Queen's University, Kingston, Ontario K7L 3N6, Canada*

³*Chemical Diagnostics and Engineering, Los Alamos National Laboratory, Los Alamos, New Mexico 87544, USA*

(Received 4 January 2015; accepted 24 February 2015; published online 19 March 2015)

In our previous work, we explored the dynamics of a dilute suspension of rigid dumbbells as a model for polymeric liquids in large-amplitude oscillatory shear flow, a flow experiment that has gained a significant following in recent years. We chose rigid dumbbells since these are the simplest molecular model to give higher harmonics in the components of the stress response. We derived the expression for the dumbbell orientation distribution, and then we used this function to calculate the shear stress response, and normal stress difference responses in large-amplitude oscillatory shear flow. In this paper, we deepen our understanding of the polymer motion underlying large-amplitude oscillatory shear flow by decomposing the orientation distribution function into its first five Fourier components (the zeroth, first, second, third, and fourth harmonics). We use three-dimensional images to explore each harmonic of the polymer motion. Our analysis includes the three most important cases: (i) nonlinear steady shear flow (where the Deborah number $\lambda\omega$ is zero and the Weissenberg number $\lambda\dot{\gamma}^0$ is above unity), (ii) nonlinear viscoelasticity (where both $\lambda\omega$ and $\lambda\dot{\gamma}^0$ exceed unity), and (iii) linear viscoelasticity (where $\lambda\omega$ exceeds unity and where $\lambda\dot{\gamma}^0$ approaches zero). We learn that the polymer orientation distribution is spherical in the linear viscoelastic regime, and otherwise tilted and peanut-shaped. We find that the peanut-shaping is mainly caused by the zeroth harmonic, and the tilting, by the second. The first, third, and fourth harmonics of the orientation distribution make only slight contributions to the overall polymer motion. © 2015 Author(s). All article content, except where otherwise noted, is licensed under a Creative Commons Attribution 3.0 Unported License. [<http://dx.doi.org/10.1063/1.4914411>]

I. INTRODUCTION

A rigid dumbbell has both length and width, the two key geometric properties of a polymer molecule, and these properties confer upon the polymer orientation (see Figures 1 and 2). By far, the most common experiment for probing the structural dynamics of polymeric liquids is oscillatory shear flow,^{1–6} and when performed at large-amplitude (Refs. 7–12; see also Section 2 of Ref. 13), this test is particularly informative. In our previous work, we have used the diffusion equation for molecular orientation to derive the expression for the orientation distribution function by expanding it in powers of the shear rate amplitude.^{37–42} This expression contains zeroth, first, second, third, and fourth harmonics. We learned that the zeroth order term in the expansion contributes only to the zeroth harmonic, the first order term to the first, the second order term to the zeroth and second, third order term to the first and third, and finally, the fourth order term to the zeroth, second, and fourth harmonics.

^{a)}Author to whom correspondence should be addressed. Electronic mail: giacomin@queensu.ca

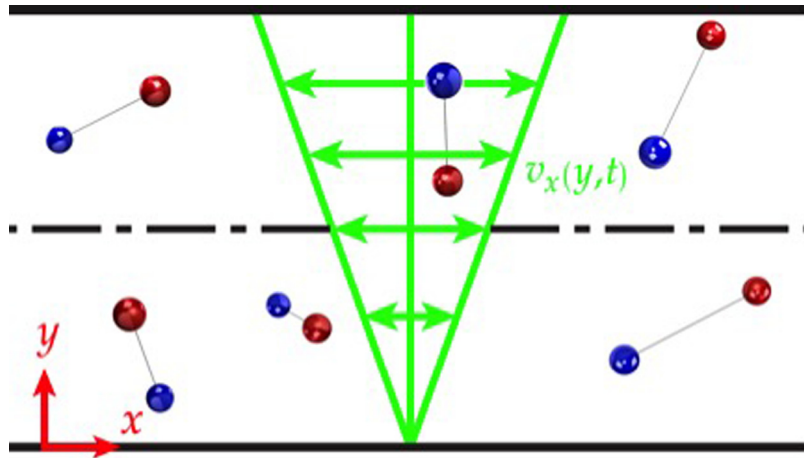


FIG. 1. Orthomorphic sketch of alternating velocity profile in oscillatory shear between stationary and moving plates [Eq. (1) or (2)]. Cartesian coordinates with origin on the stationary plate.

Table I classifies the literature on analytical solutions for orientation distribution in large-amplitude oscillatory shear flow. The connection between the components of the extra stress tensor and the orientation distribution function was established long ago,²⁸ and from this work, we know that only certain parts of the orientation distribution function contribute to each component of the extra stress tensor in simple shear flows, and that certain parts *make no contribution*. In our previous work, we have used the contributing parts to derive expressions for the shear stress and for both normal stress difference responses (see Eq. (82) of Ref. 37 and Eqs. (13) and (21) of Ref. 39). In our most recent work, we derived the full orientation distribution function, including the terms that make no contribution to the rheological responses^{40–42} (see column titled “non-contributing terms” of Table I).

In this paper, we decompose the expression for the orientation distribution function into its Fourier components (putting the Fourier coefficients under common denominators). Then, by examining each Fourier component, we see the frequency content of each of the molecular motions and examine the orientation distribution directly, by deriving expressions for the zeroth, first, second, third, and fourth harmonics of the orientation in large-amplitude oscillatory shear flow, as functions of the dimensionless frequency, $\lambda\omega$, and dimensionless shear rate amplitude, $\lambda\dot{\gamma}^0$. Our analytical solution, presented with three-dimensional color imagery, gives us insight into the molecular behaviors underpinning the observed higher harmonics in the nonlinear rheological responses.¹⁴ We thus derive new structure-property relations for the orientation distribution in large-amplitude oscillatory shear flow.

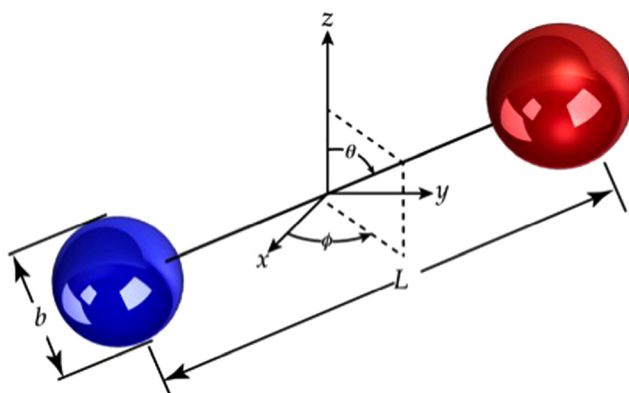


FIG. 2. The dumbbell consists of identical beads (of identical mass and of identical diameter) connected by one thin, absolutely rigid (dimensionless, massless) rod.

TABLE I. Literature on analytical solutions for orientation distribution in large-amplitude oscillatory shear flow. AS \equiv active rod suspensions; R \equiv reptation; RD \equiv rigid dumbbell; RR \equiv planar rigid ring; SK \equiv shish-kebab; \dagger \equiv mixtures; h \equiv with hydrodynamic interaction.

Model	Expansion variable	Orientation harmonic	Non-contributing terms	Fourier decomposition	Reference (correction to)
Kirkwood and Plock (1956, 1967); Plock (1957)	RD h , SK h	$\dot{\gamma}^0$	0, 2, 4, 6		28–30
Paul (1969); Paul (1970); Bharadwaj (2012)	RD h , SK h	$\dot{\gamma}^0$	0, 2, 4, 6		31–33 (28, 30)
Paul and Mazo (1969), Paul (1970)	RR	$\dot{\gamma}^0$	0, 2, 4, 6		34, 32
Bird, Warner, and Evans (1971)	RD, SK	$\dot{\gamma}^0$	0, 1, 2, 3		26
Mou and Mazo (1977)	RR	$\dot{\gamma}^0$	0, 2, 4, 6		35 (34)
Helfand and Rochefort (1982)	R †	$\dot{\gamma}^0$	See Eq. (8) in Ref. 36		36
Bird <i>et al.</i> (2014)	RD, SK	$\dot{\gamma}^0$	0, 1, 2, 3		37
Schmalzer <i>et al.</i> (2014)	RD, SK	$\dot{\gamma}^0$	0, 1, 2, 3, 4		38, 39
Schmalzer <i>et al.</i> (2014)	RD, SK	$\dot{\gamma}^0$	0, 1, 2, 3, 4	X	40–42
Bozorgi (2014); Bozorgi and Underhill (2014)	AS h	γ_0	0, 1, 2		Chapter 8 of Refs. 43; 44
This paper	RD, SK	$\dot{\gamma}^0$	0, 1, 2, 3, 4	X	X
					45

The rigid dumbbell suspension seems to mimic the behavior of polymer solutions and melts, at least qualitatively, and this seems to be because the overall orientation of the polymer chains gives the longest time constant for the polymeric liquids.

This paper concerns itself with the orientation distribution function of a suspension of rigid dumbbells, when the flow is given by a velocity field $v_x(y, t)$. We further restrict this paper to the periodic response, reached several cycles after startup of oscillatory shear, called alternance (see Section 6 of Refs. 15; 16). This work is an extension of recent articles,^{37,38} wherein part of the orientation distribution is derived using the method of Bird and Armstrong¹⁷ (see also Problem 11C.1 of Ref. 18).

A. The flow field

We are concerned here with the particular case of a homogeneous shearing flow (see Figure 1)

$$v_x = \dot{\gamma}^0 y f(t), v_y = v_z = 0, \quad (1)$$

called simple shear flow. The symbols used here and elsewhere are defined, along with their dimensions, in Tables II and III. The coefficient of proportionality between the velocity and position is $\dot{\gamma}^0 f(t)$, where the special variable f depends solely on the time. This situation can be obtained by having the flow take place between two plates placed extremely close to one another.^{19,20}

We consider only the case where $f(t) = \cos \omega t$ so that Eq. (1) becomes^{21,22}

$$v_x = \dot{\gamma}^0 y \cos \omega t; v_y = v_z = 0, \quad (2)$$

which we call oscillatory shear flow. That is, the shear rate may be written as

$$\lambda \dot{\gamma}(t) = \lambda \dot{\gamma}^0 \cos \lambda \omega t / \lambda, \quad (3)$$

in which the dimensionless shear rate $\lambda \dot{\gamma}^0$ (the Weissenberg number) and the dimensionless frequency $\lambda \omega$ (the Deborah number), appear.^{16,21,22} All orientation distribution responses calculated herein are thus referred to this sinusoidal shear rate (see Section V of Ref. 23). These

TABLE II. Dimensional variables. M = mass; L = length; t = time; T = temperature.

Velocity, i th component	L/t	v_i
Angular frequency	t^{-1}	ω
Bead center to center length of rigid dumbbell	L	L
Bead diameter	L	b
Bead friction coefficient	M/t	$\zeta \equiv 3\pi b\eta_s$
Boltzmann constant	$ML^2/t^2 T/dumbbell$	k
Cartesian coordinate, distance from stationary plate (Figure 1)	L	y
Cartesian coordinate, flow direction (Figure 1)	L	x
Cartesian coordinate, transverse to flow direction (Figure 1)	L	z
Gap	L	h
Relaxation time of fluid	t	λ
Shear rate amplitude	t^{-1}	$\dot{\gamma}^0$
Solvent viscosity	M/Lt	η_s
Temperature	T	T
Time	t	t

dimensionless groups contain the characteristic time constant λ for which the dilute suspension of rigid dumbbells in a Newtonian solvent of viscosity η_s is

$$\lambda \equiv \frac{\zeta L^2}{12kT} = \frac{(3\pi\eta_s b)L^2}{12kT} \quad (4)$$

and for rigid multibead-rods:

$$\lambda_N = \frac{\zeta L^2 N(N+1)}{72(N-1)kT}, \quad (5)$$

where N is the number of equally spaced beads on the rod of length L , T is absolute temperature, k is Boltzmann's constant, ζ is the bead friction factor, given by Stokes' law, and b is the diameter of each of the beads of the dumbbell (see Figure 2). Equation (3) applies for continuum, and thus cannot apply when the gap, h , approaches the size of the molecules, L , or when $L/h \ll 1$. For a detailed study of small-amplitude oscillatory shear for a rigid dumbbell suspension in confined gaps, see Section 5 of Ref. 24 or Section 2.3.3 of Ref. 25.

In this paper, we consider the special case of Eq. (3) where higher harmonics arise in both the shear stress and in the normal stress difference responses.

TABLE III. Dimensionless variables and groups.

Azimuthal angle	ϕ
Deborah number squared	$W \equiv (\lambda\omega)^2$
Deborah number, oscillatory shear	$\lambda\omega$
Number of equally spaced beads on a rod of length ($L - b$)	N
Number of harmonic	n
Orientation distribution	$\psi(\theta, \phi, t)$
i th term of orientation distribution expansion	$\psi_i(\theta, \phi, t)$
Orientation distribution, Fourier component, in-phase with $\cos n\omega t$	$\psi'_n(\theta, \phi)$
Orientation distribution, Fourier component, out-of-phase with $\cos n\omega t$	$\psi''_n(\theta, \phi)$
Polar angle	θ
Time dependent part of shear rate for velocity profile, assumed linear in y [Eq. (1)]	$f(t)$
Weissenberg number, oscillatory shear	$\lambda\dot{\gamma}^0$

B. Orientation distribution function

For simple shear flow, the *diffusion equation* for the orientation distribution function $\psi(\theta, \phi, t)$ is given by (see Eq. (5.1) of Ref. 26, Eq. (14.4–1) of Ref. 27)

$$6\lambda \frac{\partial \psi}{\partial t} = \left[\frac{1}{S} \frac{\partial}{\partial \theta} \left(S \frac{\partial \psi}{\partial \theta} \right) + \frac{1}{S^2} \frac{\partial^2 \psi}{\partial \phi^2} \right] - 6\lambda \dot{\gamma} \left[\frac{sc}{S} \frac{\partial}{\partial \theta} (S^2 C \psi) - \frac{\partial}{\partial \phi} (s^2 \psi) \right], \quad (6)$$

where $\lambda \dot{\gamma}$ is the dimensionless oscillatory shear rate [given by Eq. (3)]. In Eq. (6), we use the abbreviations $S \equiv \sin \theta$, $C \equiv \cos \theta$, $s \equiv \sin \phi$, and $c \equiv \cos \phi$. For ψ , we adhere to the definition of Bird-Warner-Evans²⁶ which differs from that of Refs. 18 and 27. The relation between the distribution function used here, ψ , and the symbol used in the first¹⁸ and second²⁷ editions of *Dynamics of Polymeric Liquids* is (see footnote 1 on p. 524 of Ref. 18)

$$\psi_{DPL,1e} = \psi_{DPL,2e} = \psi \sin \theta. \quad (7)$$

Also, the symbol for the distribution function used here is ψ that used in the second edition of *Dynamics of Polymeric Liquids*²⁷ is f .

The dumbbell orientation is thus given in terms of the spherical coordinates θ and ϕ which are defined in Figure 2. When the fluid is at rest, all orientations are equally likely, and ψ is equal to a normalization constant, $1/4\pi$, so that

$$\int_0^{2\pi} \int_0^\pi \psi(\theta, \phi, t) \sin \theta d\theta d\phi = 1. \quad (8)$$

In other words, when the fluid is at rest, $\psi(\theta, \phi)$ is spherically symmetric. Although the orientation distribution function for rigid dumbbell suspension has not been measured directly, its implications for rheological behaviors have been verified experimentally. Reasonable qualitative behaviors for oscillatory shear flow are obtained for amplitudes both small²⁶ and large.^{37,38}

II. METHOD

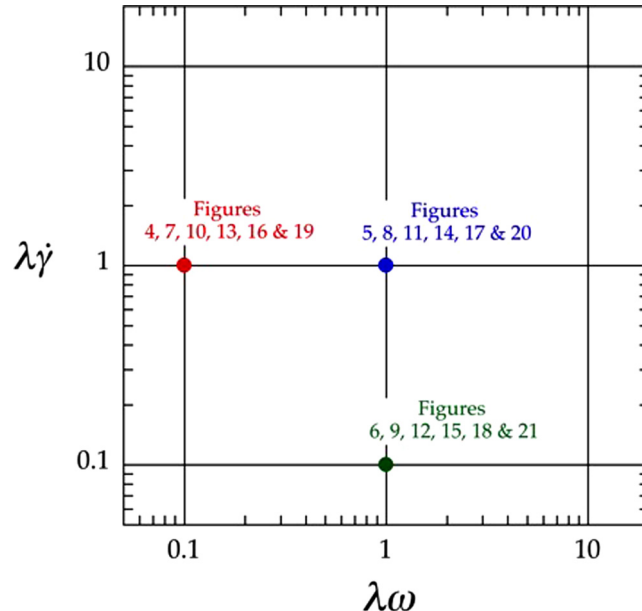
Schmalzer and Giacomin^{40–42} recently solved Eq. (6) for large-amplitude oscillatory shear flow, including terms that do not contribute to the rheological responses, using the method of Bird and Armstrong.¹⁷ This solution has the form

$$\psi(\theta, \phi, t) = \frac{1}{4\pi} \left[1 + (6\lambda \dot{\gamma}^0) \psi_1(\theta, \phi, t) + (6\lambda \dot{\gamma}^0)^2 \psi_2(\theta, \phi, t) + (6\lambda \dot{\gamma}^0)^3 \psi_3(\theta, \phi, t) + (6\lambda \dot{\gamma}^0)^4 \psi_4(\theta, \phi, t) + \dots \right], \quad (9)$$

where ψ_1 through ψ_4 are given by Eqs. (36), (44), (52), and (61) of Ref. 40. In this paper, we undertake the laborious Fourier decomposition of these expressions for ψ_1 through ψ_4 , putting the resulting Fourier coefficients under common denominators. By *Fourier decomposition*, we mean rewriting Eq. (9) as the Fourier series

$$\psi(\theta, \phi, t) = \sum_{n=0}^{\infty} [\psi'_n \cos n\omega t + \psi''_n \sin n\omega t], \quad (10)$$

where ψ'_n and ψ''_n are the Fourier coefficients of the orientation distribution function respectively in-phase and out-of-phase with $\cos n\omega t$. This Fourier decomposition, and finding of common denominators is straightforward, but tedious. To prevent introducing errors, we thus checked each result given below numerically by comparing the expressions before and after the Fourier decomposition to 16 significant figures. Specifically, Eq. (9) with Eqs. (36), (44), (52), and (61) of Ref. 40 checks with Eq. (10) with Eqs. (11)–(20) to at least 16 significant figures.

FIG. 3. Conditions of $\lambda\omega$ and $\lambda\dot{\gamma}^0$ for Figures 4–21.

III. RESULTS

From the results given below, we see that in oscillatory shear flow the polymer orientation distribution decomposes into both even (starting with the zeroth) and odd harmonics. We identify the even harmonics of the polymer motion with the differences in the normal components of the extra stress tensor, whose Fourier components are also all even. We can further identify the odd harmonics of the orientation with the yx -component of the extra stress tensor (called the shear stress), whose Fourier components are also all odd valued. To help the reader navigate Figures 4–18 (Multimedia view), we provide Figure 3 showing the relevant conditions of $\lambda\omega$ and $\lambda\dot{\gamma}^0$. Our analysis includes the three most important cases: (i) nonlinear steady shear flow (where the Deborah number $\lambda\omega$ is near zero and the Weissenberg number $\lambda\dot{\gamma}^0$ is unity) [Figures 4, 7 (Multimedia view), 10 (Multimedia view), 13 (Multimedia view), and 16 (Multimedia view)], (ii) nonlinear viscoelasticity (where both $\lambda\omega$ and $\lambda\dot{\gamma}^0$ exceed unity) [Figures 5, 8 (Multimedia view), 11 (Multimedia view), 14 (Multimedia view), and 17 (Multimedia view)], and (iii) nearly linear viscoelasticity (where $\lambda\omega$ is unity and where $\lambda\dot{\gamma}^0$ approaches zero) [Figures 6, 9 (Multimedia view), 12 (Multimedia view), 15 (Multimedia view), and 18 (Multimedia view)].

A. Zeroth harmonic

The Fourier coefficient of the zeroth harmonic of the orientation distribution function for a rigid dumbbell suspension in large-amplitude oscillatory shear flow is given by

$$\psi'_0 = \frac{1}{4\pi} \left[\begin{array}{l} 1 - (6\lambda\dot{\gamma}^0)^2 \left\{ \frac{\left[-\frac{3}{4}(15C^4 + 30C^2 - 7) - 30(1 - C^2)c_2 + \frac{315}{28}(1 - C^2)^2 c_4 \right]}{1440(1 + W)} \right\} \\ - (6\lambda\dot{\gamma}^0)^4 \left\{ \frac{\left[(1161W^3 + 14769W^2 + 74200W + 40000)(3C^2 - 1) \right.} {221760(W + 1)^2(4W + 1)(9W + 25)(9W + 100)} \\ \left. + 11(1107W^3 + 19303W^2 + 60050W + 28750)(1 - C^2)c_2 \right] \end{array} \right]. \quad (11)$$

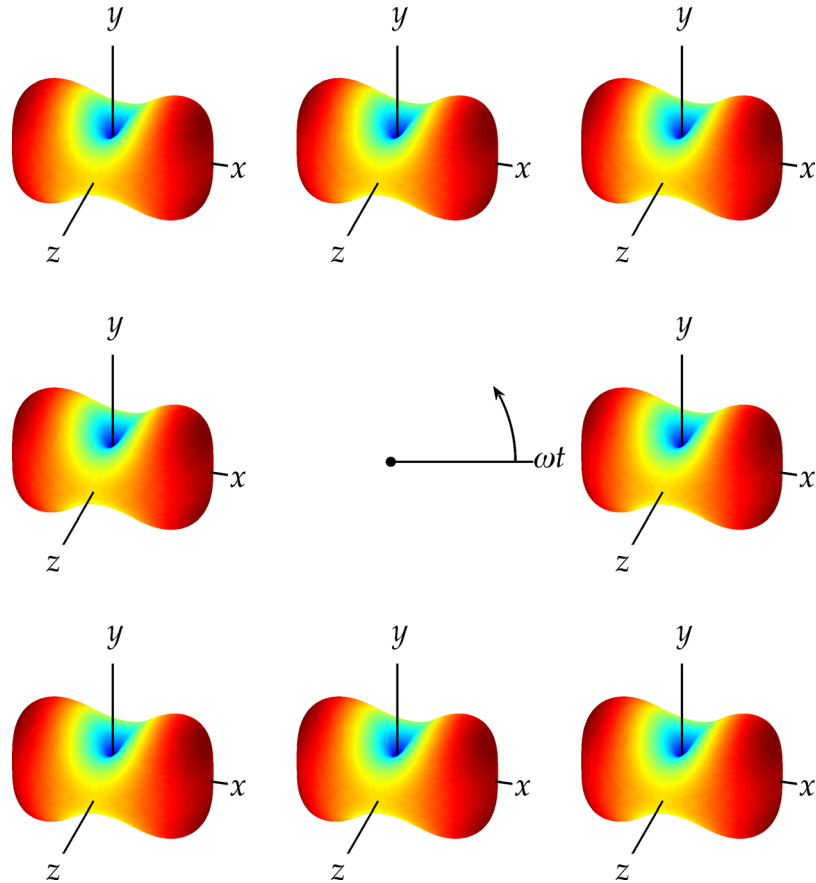


FIG. 4. Zeroth harmonic of ψ , ψ'_0 , from Eq. (11), over a complete alternant cycle of $\omega t = 0$ to $\omega t = 2\pi$, with $\lambda\omega = 0.1$ and $\lambda\dot{\gamma}^0 = 1$. Only ψ_2 and ψ_4 contribute to these orientations. Nonlinear steady shear flow regime.

Figures 4–6 illustrate the time steady orientation induced by the oscillatory shear deformation, and predicted by Eq. (11), as we progress from nonlinear steady shear flow to nonlinear viscoelasticity and to linear viscoelasticity (see this progression illustrated in Figure 3). In Figures 4 and 5, we see the origins of the peanut-shapes that we find in the overall orientation distribution (Figures 19 and 20). The sphericity of Figure 6 reflects the close proximity of the polymeric liquid structure in the linear viscoelastic region to the polymeric liquid at rest.

B. First harmonic

The Fourier coefficient of the first harmonic of orientation distribution function for a rigid dumbbell suspension in large-amplitude oscillatory shear flow is given by

$$\psi'_1 = \frac{1}{4\pi} \left[(6\lambda\dot{\gamma}^0) \frac{1}{4} (1 - C^2) s_2 \left(\frac{1}{1 + W} \right) + (6\lambda\dot{\gamma}^0)^3 \left\{ \begin{aligned} & \left[\begin{aligned} & -\frac{1}{3920} (75 - 37W)(W + 49)(4W + 1)(9W + 100) \\ & -\frac{15}{68992} (97W + 860)(W + 1)(W + 49)(9W + 25)(7C^2 - 1) \\ & +\frac{7}{67584} (525 - 19W)(W + 1)(4W + 1)(9W + 100)(33C^4 - 18C^2 + 1) \end{aligned} \right] s_2 \\ & + \left[\begin{aligned} & \frac{5}{256} (160 - W)(W + 1)(W + 49)(9W + 25)(1 - C^2)s_4 \\ & -\frac{7}{6144} (525 - 19W)(W + 1)(4W + 1)(9W + 100)(1 - C^2)^2 s_6 \end{aligned} \right] (1 - C^2) \end{aligned} \right\} \right], \quad (12)$$

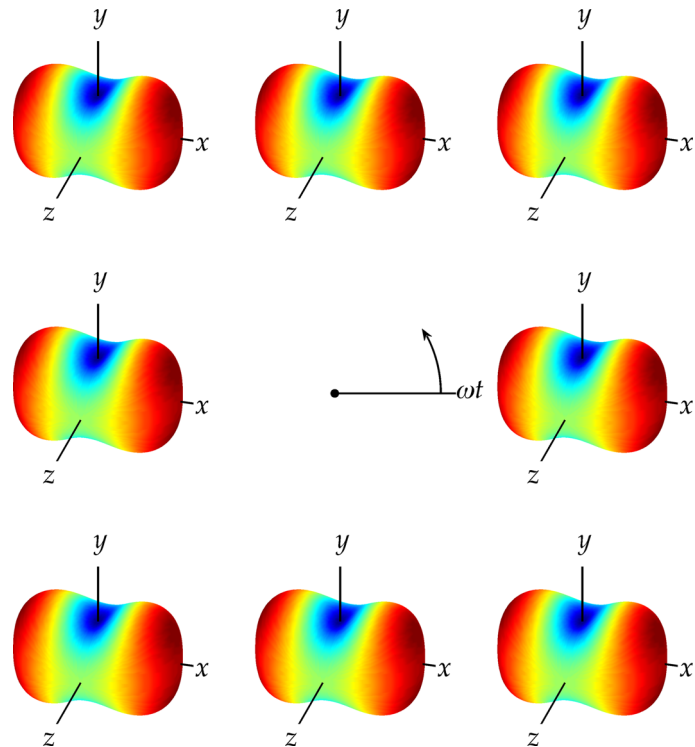


FIG. 5. Zeroth harmonic of ψ, ψ'_0 , from Eq. (11), over a complete alternant cycle of $\omega t = 0$ to $\omega t = 2\pi$, with $\lambda\omega = 1$ and $\lambda\dot{\gamma}^0 = 1$. Only ψ_2 and ψ_4 contribute to these orientations. Nonlinear viscoelastic regime.

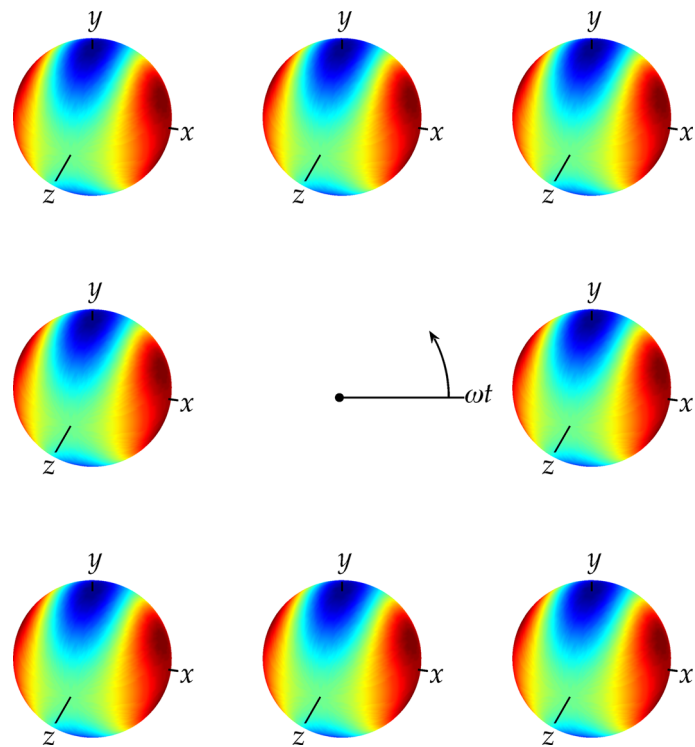


FIG. 6. Zeroth harmonic of ψ, ψ'_0 , from Eq. (11), over a complete alternant cycle of $\omega t = 0$ to $\omega t = 2\pi$, with $\lambda\omega = 1$ and $\lambda\dot{\gamma}^0 = 0.1$. Only ψ_2 and ψ_4 contribute to these orientations. Nearly linear viscoelastic regime.

and

$$\psi''_1 = \frac{1}{4\pi} \left[(6\lambda\dot{\gamma}^0) \frac{1}{4} (1 - C^2) s_2 \left(\frac{1}{1 + W} \right) + (6\lambda\dot{\gamma}^0)^3 \left\{ \begin{aligned} & \left[\begin{aligned} & -\frac{1}{1680}(W+49)(9W+100)(153W^2+757W+460) \\ & -\frac{45}{68992}(25W+256)(W+1)(W+49)(9W+25)(7C^2-1) \\ & +\frac{7}{67584}(3W+355)(W+1)(4W+1)(9W+100)(33C^4-18C^2+1) \\ & +\frac{3}{256}(13W+230)(W+1)(W+49)(9W+25)(1-C^2)s_4 \\ & -\frac{7}{6144}(3W+355)(W+1)(4W+1)(9W+100)(1-C^2)^2s_6 \end{aligned} \right] s_2 \end{aligned} \right\} (1 - C^2) \right\} \lambda\omega. \quad (13)$$

Figures 7 (Multimedia view)–9 (Multimedia view) illustrate the orientation distribution associated with the polymer motions arising at the test frequency ω that are induced by the oscillatory shear deformation, and predicted by Eqs. (12) and (13), as we progress from nonlinear steady shear flow to nonlinear viscoelasticity and to linear viscoelasticity (see this progression illustrated in Figure 3). In Figure 9 (Multimedia view), we see the only slight disturbance of the spherical orientation distribution that exists for a polymeric liquid at rest. Furthermore, comparing Figure 7 (Multimedia view) with Figure 19, or Figure 8 (Multimedia view) with Figure 20, we learn that even for the nonlinear behaviors, the first harmonic is hardly reshaping the orientation distribution established by the zeroth harmonic. So the tilting of the peanut-shapes in Figures 19 and 20 is not caused by the first harmonic.

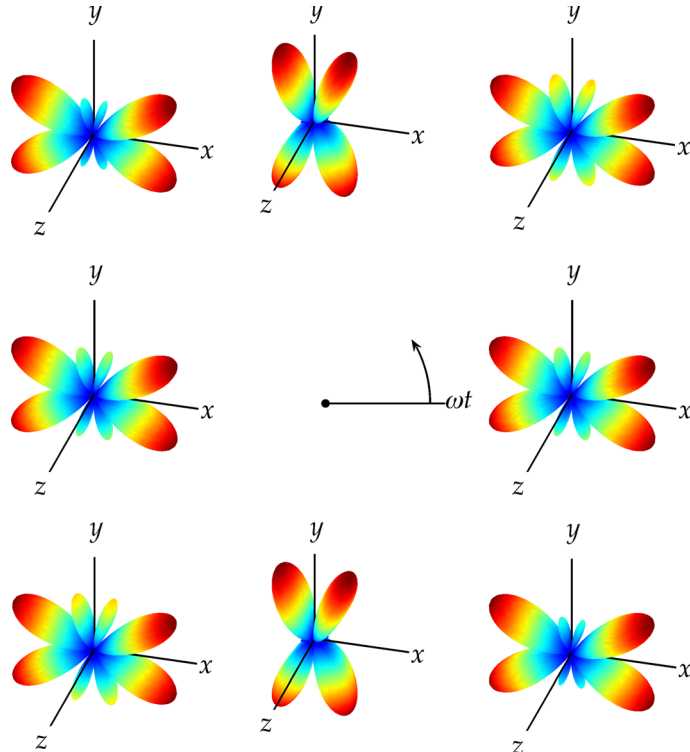


FIG. 7. First harmonic of ψ , $\psi'_1 \cos \omega t + \psi''_1 \sin \omega t$ with Eqs. (12) and (13), over a complete alternant cycle of $\omega t = 0$ to $\omega t = 2\pi$, with $\lambda\omega = 0.1$ and $\lambda\dot{\gamma}^0 = 1$. Only ψ_1 and ψ_3 contribute to these orientations. Nonlinear steady shear flow regime. Corresponding animation can be downloaded from online article. (Multimedia view) [URL: <http://dx.doi.org/10.1063/1.4914411.1>]

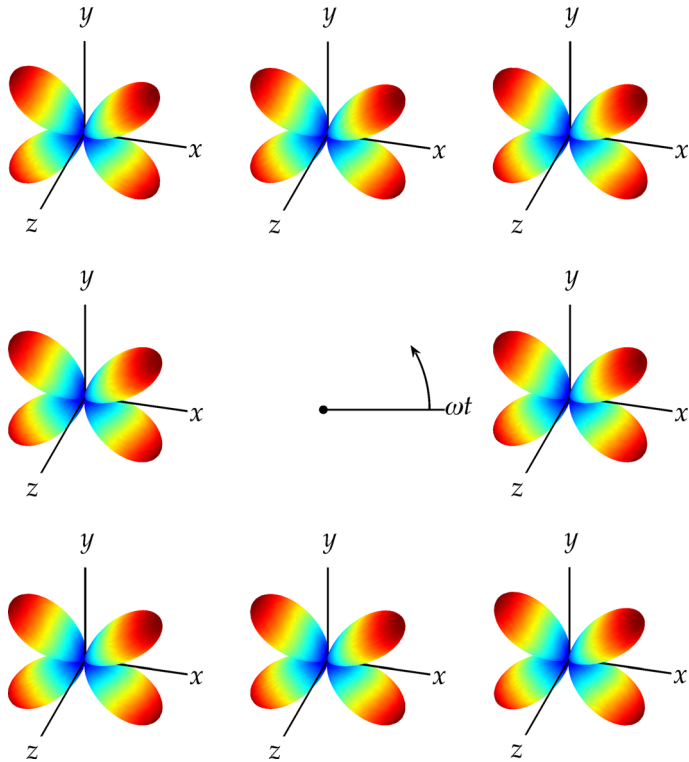


FIG. 8. First harmonic of ψ , $\psi'_1 \cos \omega t + \psi''_1 \sin \omega t$ with Eqs. (12) and (13), over a complete alternant cycle of $\omega t = 0$ to $\omega t = 2\pi$, with $\lambda\omega = 1$ and $\lambda\dot{\gamma}^0 = 1$. Only ψ_1 and ψ_3 contribute to these orientations. Nonlinear viscoelastic regime. Corresponding animation can be downloaded from online article. (Multimedia view) [URL: <http://dx.doi.org/10.1063/1.4914411.2>]

C. Second harmonic

The Fourier coefficient of the second harmonic of the orientation distribution function for a rigid dumbbell suspension in large-amplitude oscillatory shear flow is given by

$$\psi'_2 = \frac{1}{4\pi} \left[\begin{array}{l} (6\lambda\dot{\gamma}^0)^2 \left\{ \begin{array}{l} \frac{24}{7}(3C^2 - 1)(1 - 2W)(25 + 9W) \\ -\frac{9}{28}(35C^4 - 30C^2 + 3)(10 - 6W)(1 + 4W) \\ -24(1 - C^2)(1 - 2W)(25 + 9W)c_2 \\ +\frac{315}{28}(1 - C^2)^2(10 - 6W)(1 + 4W)c_4 \end{array} \right\} \\ -\frac{(72)16(1 + W)(1 + 4W)(25 + 9W)}{} \end{array} \right] \\ + (6\lambda\dot{\gamma}^0)^4 \left\{ \begin{array}{l} \left(27917501148W^7 + 395970769863W^6 + 1359686945763W^5 \right. \\ \left. + 1401100327677W^4 + 389057165809W^3 + 45722628300W^2 \right) (3C^2 - 1) \\ -\frac{22856340000W - 1568000000}{6519744(W + 1)^3(4W + 1)(9W + 1)(9W + 25)(9W + 100)(16W + 1)(81W + 100)} \\ \left(506797884W^7 + 6027824709W^6 + 1947775889W^5 \right. \\ \left. + 19601882811W^4 + 5251665787W^3 + 424722600W^2 \right) (1 - C^2)c_2 \\ +\frac{-340140000W - 23000000}{120960(W + 1)^3(4W + 1)(9W + 1)(9W + 25)(16W + 1)(81W + 100)} \end{array} \right\}, \quad (14)$$

and

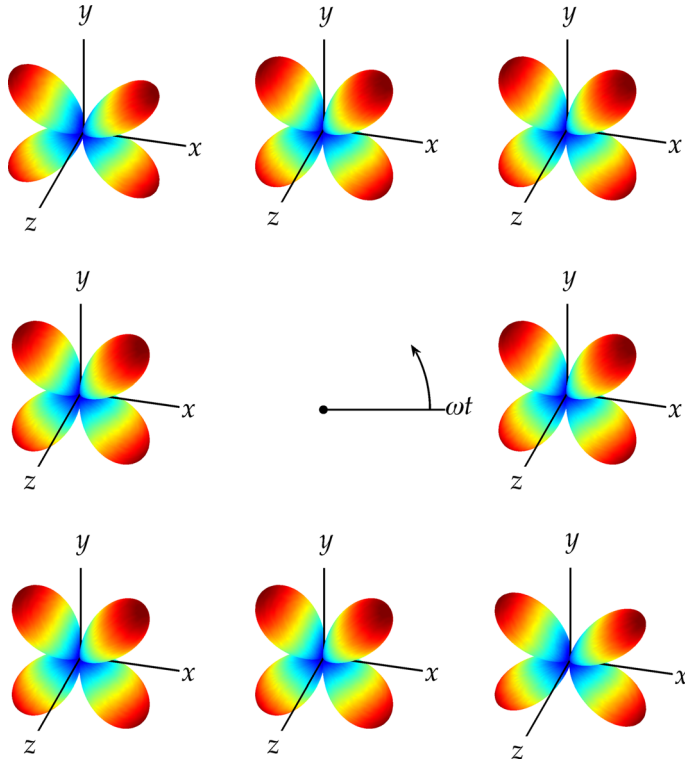


FIG. 9. First harmonic of $\psi, \psi'_1 \cos \omega t + \psi''_1 \sin \omega t$ with Eqs. (12) and (13), over a complete alternant cycle of $\omega t = 0$ to $\omega t = 2\pi$, with $\lambda\omega = 1$ and $\lambda\dot{\gamma}^0 = 0.1$. Only ψ_1 and ψ_3 contribute to these orientations. Nearly linear viscoelastic regime. Corresponding animation can be downloaded from online article. (Multimedia view) [URL: <http://dx.doi.org/10.1063/1.4914411.3>]

$$\psi''_2 = \frac{1}{4\pi} \left[\begin{array}{l} \left(6\lambda\dot{\gamma}^0 \right)^2 \left\{ -\frac{\left[\begin{array}{l} \frac{9}{7}(3C^2 - 1)(25 + 9W) - \frac{9}{14}(35C^4 - 30C^2 + 3)(1 + 4W) \\ - 9(1 - C^2)(25 + 9W)c_2 + \frac{630}{28}(1 - C^2)^2(1 + 4W)c_4 \end{array} \right]}{144(1 + W)(1 + 4W)(25 + 9W)} \right\} \\ + \left(6\lambda\dot{\gamma}^0 \right)^4 \left[\begin{array}{l} \left(\begin{array}{l} 4554095076W^7 + 54922330017W^6 + 62656044453W^5 \\ - 366082940052W^4 - 649050340979W^3 - 299118407355W^2 \\ - 75936742500W - 3787700000 \end{array} \right)(3C^2 - 1) \\ \frac{325987320(W + 1)^3(4W + 1)(9W + 1)(9W + 25)(9W + 100)(16W + 1)(81W + 100)}{+ (6\lambda\dot{\gamma}^0)^4 \left[\begin{array}{l} \left(\begin{array}{l} 73929348W^7 + 725310531W^6 + 487357884W^5 \\ - 5792477481W^4 - 9601088132W^3 - 4427460420W^2 \\ - 1076466750W - 53975000 \end{array} \right)(1 - C^2)c_2 \\ + \frac{60480(W + 1)^3(4W + 1)(9W + 1)(9W + 25)(9W + 100)(16W + 1)(81W + 100)}{ \right] } \end{array} \right] \end{array} \right] \lambda\omega. \quad (15)$$

Figures 10 (Multimedia view)–12 (Multimedia view) illustrate the orientation distribution associated with the polymer motions arising at twice the test frequency, 2ω , which are induced by the oscillatory shear deformation, and predicted by Eqs. (14) and (15), as we progress from nonlinear steady shear flow to nonlinear viscoelasticity and to linear viscoelasticity (see this progression illustrated in Figure 3). Comparing Figure 10 (Multimedia view) with Figure 19, or Figure 11 (Multimedia view) with Figure 20, we learn that the tilt of the peanuts in the overall orientation distributions for nonlinear behaviors is mainly due to the second harmonic. Furthermore, we see that the second harmonic contributes to orientation along the axes, whereas the first harmonic predicts polymer orientation away from the axes in the x, y -plane.

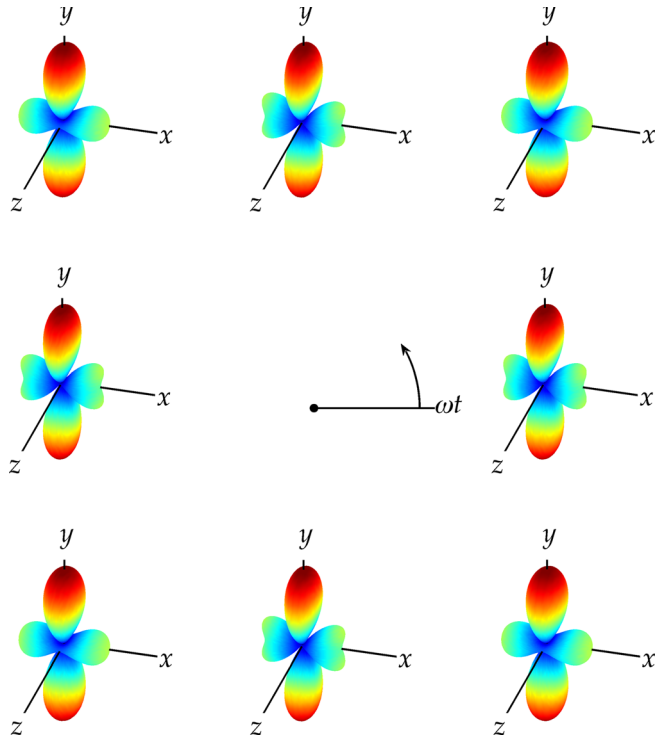


FIG. 10. Second harmonic of ψ , $\psi'_2 \cos 2\omega t + \psi''_2 \sin 2\omega t$ with Eqs. (14) and (15), over a complete alternant cycle of $\omega t = 0$ to $\omega t = 2\pi$, with $\lambda\omega = 0.1$ and $\lambda\dot{\gamma}^0 = 1$. Only ψ_2 and ψ_4 contribute to these orientations. Nonlinear steady shear flow regime. Corresponding animation can be downloaded from online article. (Multimedia view) [URL: <http://dx.doi.org/10.1063/1.4914411.4>]

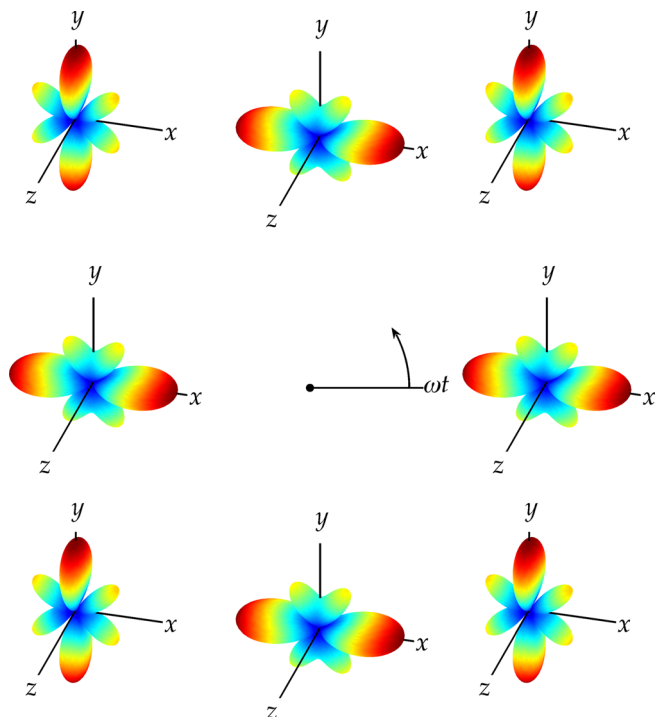


FIG. 11. Second harmonic of ψ , $\psi'_2 \cos 2\omega t + \psi''_2 \sin 2\omega t$ with Eqs. (14) and (15), over a complete alternant cycle of $\omega t = 0$ to $\omega t = 2\pi$, with $\lambda\omega = 1$ and $\lambda\dot{\gamma}^0 = 1$. Only ψ_2 and ψ_4 contribute to these orientations. Nonlinear viscoelastic regime. Corresponding animation can be downloaded from online article. (Multimedia view) [URL: <http://dx.doi.org/10.1063/1.4914411.5>]

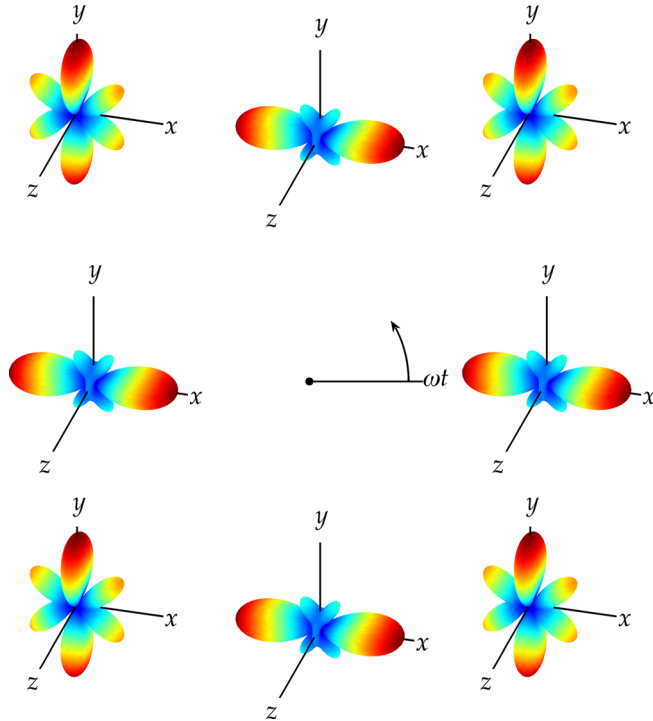


FIG. 12. Second harmonic of ψ , $\psi_2' \cos 2\omega t + \psi_2'' \sin 2\omega t$ with Eqs. (14) and (15), over a complete alternant cycle of $\omega t = 0$ to $\omega t = 2\pi$, with $\lambda\omega = 1$ and $\lambda\dot{\gamma}^0 = 0.1$. Only ψ_2 and ψ_4 contribute to these orientations. Nearly linear viscoelastic regime. Corresponding animation can be downloaded from online article. (Multimedia view) [URL: <http://dx.doi.org/10.1063/1.4914411.6>]

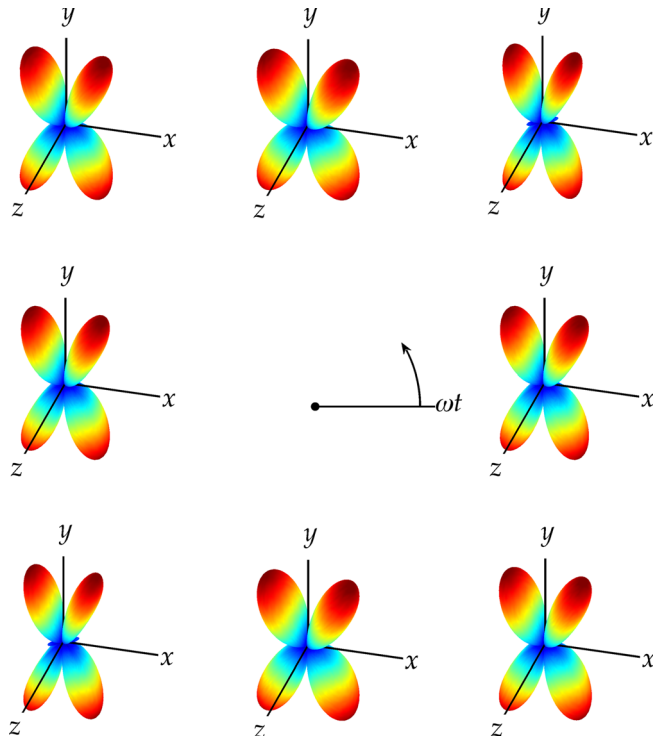


FIG. 13. Third harmonic of ψ , $\psi_3' \cos 3\omega t + \psi_3'' \sin 3\omega t$ with Eqs. (16) and (17), over a complete alternant cycle of $\omega t = 0$ to $\omega t = 2\pi$, with $\lambda\omega = 0.1$ and $\lambda\dot{\gamma}^0 = 1$. Only ψ_3 contributes to these orientations. Nonlinear steady shear flow regime. Corresponding animation can be downloaded from online article. (Multimedia view) [URL: <http://dx.doi.org/10.1063/1.4914411.7>]

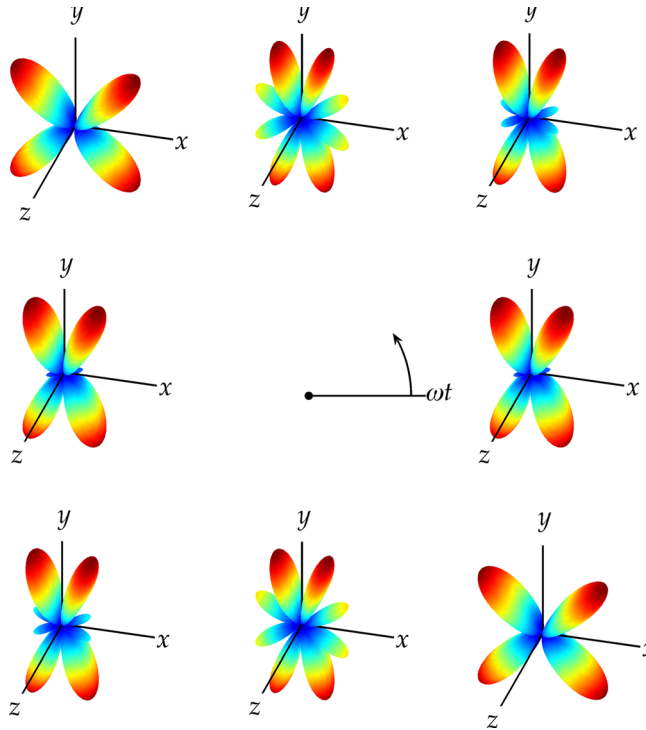


FIG. 14. Third harmonic of ψ , $\psi'_3 \cos 3\omega t + \psi''_3 \sin 3\omega t$ with Eqs. (16) and (17), over a complete alternant cycle of $\omega t = 0$ to $\omega t = 2\pi$, with $\lambda\omega = 1$ and $\lambda\dot{\gamma}^0 = 1$. Only ψ_3 contributes to these orientations. Nonlinear viscoelastic regime. Corresponding animation can be downloaded from online article. (Multimedia view) [URL: <http://dx.doi.org/10.1063/1.4914411.8>]

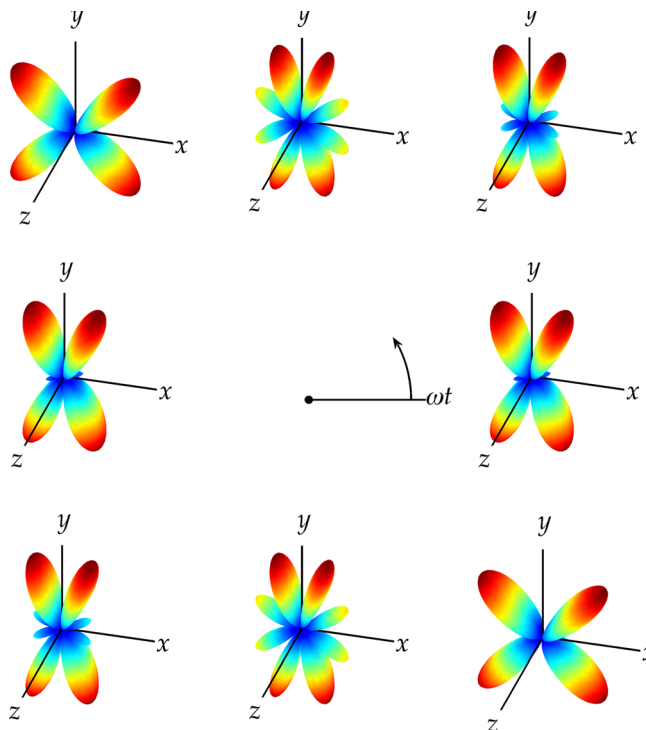


FIG. 15. Third harmonic of ψ , $\psi'_3 \cos 3\omega t + \psi''_3 \sin 3\omega t$ with Eqs. (16) and (17), over a complete alternant cycle of $\omega t = 0$ to $\omega t = 2\pi$, with $\lambda\omega = 1$ and $\lambda\dot{\gamma}^0 = 0.1$. Only ψ_3 contributes to these orientations. Nearly linear viscoelastic regime. Corresponding animation can be downloaded from online article. (Multimedia view) [URL: <http://dx.doi.org/10.1063/1.4914411.9>]

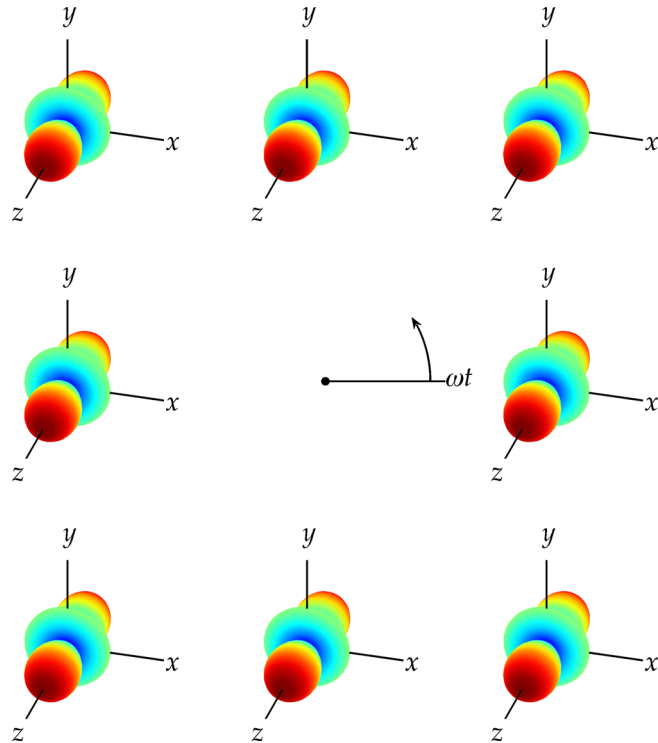


FIG. 16. Fourth harmonic of $\psi, \psi'_4 \cos 4\omega t + \psi''_4 \sin 4\omega t$ with Eqs. (19) and (20), over a complete alternant cycle of $\omega t = 0$ to $\omega t = 2\pi$, with $\lambda\omega = 0.1$ and $\lambda\dot{\gamma}^0 = 1$. Only ψ_4 contributes to these orientations. Nonlinear steady shear flow regime. Corresponding animation can be downloaded from online article. (Multimedia view) [URL: <http://dx.doi.org/10.1063/1.4914411.10>]

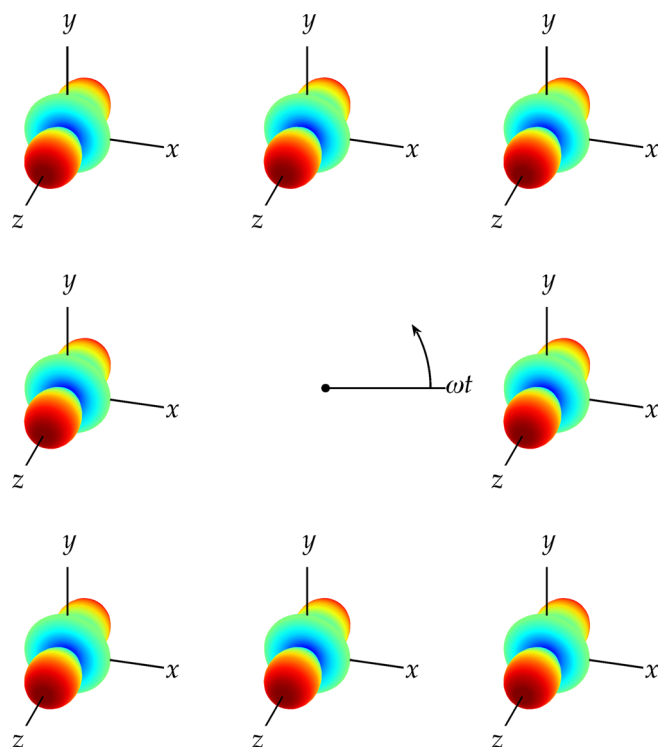


FIG. 17. Fourth harmonic of $\psi, \psi'_4 \cos 4\omega t + \psi''_4 \sin 4\omega t$ with Eqs. (19) and (20), over a complete alternant cycle of $\omega t = 0$ to $\omega t = 2\pi$, with $\lambda\omega = 1$ and $\lambda\dot{\gamma}^0 = 1$. Only ψ_4 contributes to these orientations. Nonlinear viscoelastic regime. Corresponding animation can be downloaded from online article. (Multimedia view) [URL: <http://dx.doi.org/10.1063/1.4914411.11>]

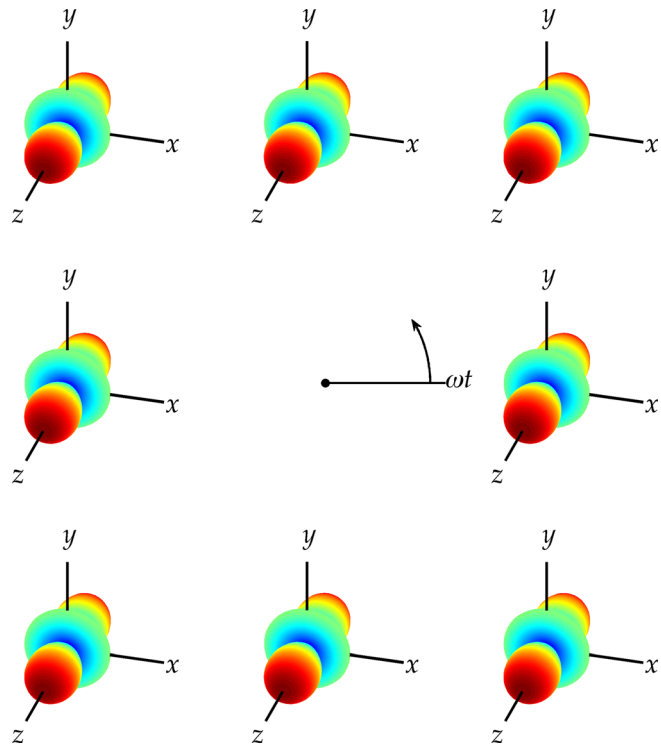


FIG. 18. Fourth harmonic of ψ , $\psi'_4 \cos 4\omega t + \psi''_4 \sin 4\omega t$ with Eqs. (19) and (20), over a complete alternant cycle of $\omega t = 0$ to $\omega t = 2\pi$, with $\lambda\omega = 1$ and $\lambda\dot{\gamma}^0 = 0.1$. Only ψ_4 contributes to these orientations. Nearly linear viscoelastic regime. Corresponding animation can be downloaded from online article. (Multimedia view) [URL: <http://dx.doi.org/10.1063/1.4914411.12>]

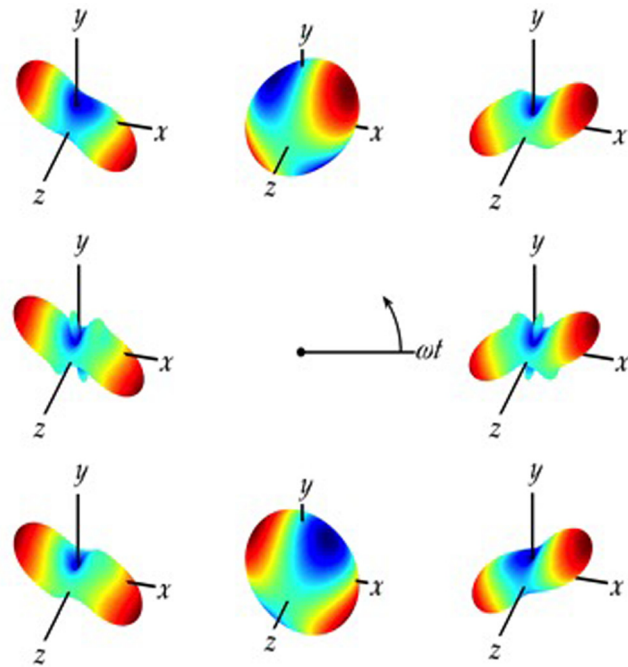


FIG. 19. Sum of first five harmonics of ψ , $\sum_{n=0}^4 [\psi'_n \cos n\omega t + \psi''_n \sin n\omega t]$ with Eqs. (11)–(20), over a complete alternant cycle of $\omega t = 0$ to $\omega t = 2\pi$, with $\lambda\omega = 0.1$ and $\lambda\dot{\gamma}^0 = 1$. Nonlinear steady shear flow regime.

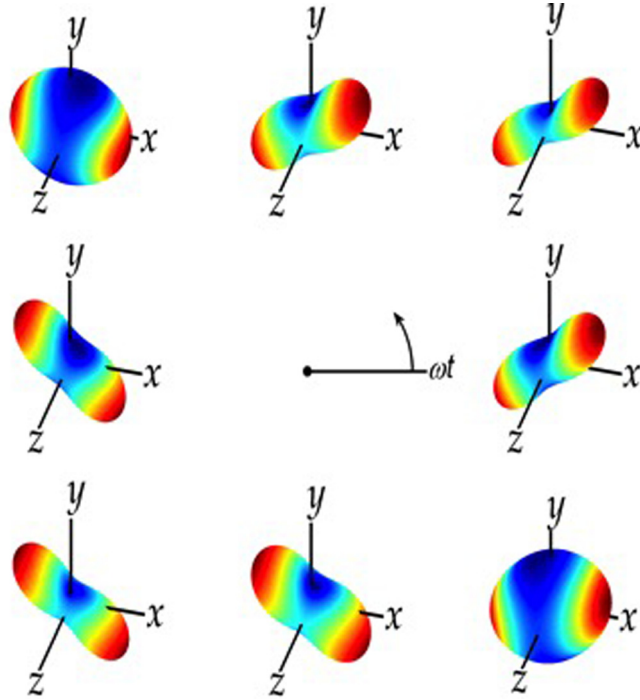


FIG. 20. Sum of first five harmonics of ψ , $\sum_{n=0}^4 [\psi'_n \cos n\omega t + \psi''_n \sin n\omega t]$ with Eqs. (11)–(20), over a complete alternant cycle of $\omega t = 0$ to $\omega t = 2\pi$, with $\lambda\omega = 1$ and $\lambda\dot{\gamma}^0 = 1$. Nonlinear viscoelastic regime.

D. Third harmonic

The Fourier coefficient of the third harmonic of orientation distribution function for a rigid dumbbell suspension in large-amplitude oscillatory shear flow is given by

$$\psi'_3 = \left\{ \frac{\left[\begin{array}{l} \frac{1}{2016}(603W^2 + 892W - 95)(9W + 49)(81W + 100) \\ + \frac{5}{9856}(19W - 5)(9W + 1)(9W + 49)(81W + 100)(7C^2 - 1) \\ + \frac{36}{13903}(7 - 9W)(4W + 1)(9W + 1)(81W + 100)(33C^4 - 18C^2 + 1) \\ - \frac{5}{768}(1647W^2 + 791W - 400)(9W + 1)(9W + 49)(1 - C^2)s_4 \\ + \frac{175}{6144}(9W - 7)(4W + 1)(9W + 1)(81W + 100)(1 - C^2)^2 s_6 \end{array} \right] s_2}{(W + 1)(4W + 1)(9W + 1)(9W + 25)(9W + 49)(81W + 100)} \right\} (1 - C^2), \quad (16)$$

and

$$\psi''_3 = \left\{ \frac{\left[\begin{array}{l} \frac{1}{336}(9W + 49)(81W + 100)(45W^2 + 17W - 92) \\ + \frac{15}{4928}(W - 3)(9W + 1)(9W + 49)(81W + 100)(7C^2 - 1) \\ + \frac{35}{67584}(71 - 9W)(4W + 1)(9W + 1)(81W + 100)(33C^4 - 18C^2 + 1) \\ - \frac{5}{128}(81W^2 - 220W - 225)(9W + 1)(9W + 49)(1 - C^2)s_4 \\ + \frac{35}{6144}(9W - 71)(4W + 1)(9W + 1)(81W + 100)(1 - C^2)^2 s_6 \end{array} \right] s_2}{(W + 1)(4W + 1)(9W + 1)(9W + 25)(9W + 49)(81W + 100)} \right\} \lambda\omega. \quad (17)$$

Figures 13 (Multimedia view)–15 (Multimedia view) illustrate the orientation distribution associated with the polymer motions arising at thrice the test frequency, 3ω , which are induced by the oscillatory shear deformation, and predicted by Eqs. (16) and (17), as we progress from nonlinear steady shear flow to nonlinear viscoelasticity and to linear viscoelasticity (see this progression illustrated in Figure 3). In Figure 15 (Multimedia view), we see the only slight disturbance of the spherical orientation distribution that exists for a polymeric liquid at rest. Furthermore, comparing Figure 13 (Multimedia view) with Figure 19, or Figure 15 (Multimedia view) with Figure 20, we learn that even for the nonlinear behaviors, the third harmonic is hardly reshaping the orientation distribution established by the zeroth harmonic. So the tilting of the peanut-shapes in Figures 19 and 20 is not caused by the first harmonic. Finally, comparing results for the first harmonic (Figures 7 (Multimedia view)–9 (Multimedia view)) with results for the third (Figure 13 (Multimedia view)–15 (Multimedia view)), we see that

$$[\psi'_1(\theta, \phi)\cos\omega t + \psi''_1(\theta, \phi)\sin\omega t] \propto [\psi'_3\left(\theta + \frac{\pi}{2}, \phi\right)\cos 3\omega t + \psi''_3\left(\theta + \frac{\pi}{2}, \phi\right)\sin 3\omega t], \quad (18)$$

so that the slight contributions to orientation made with the first and third harmonics seem to be, at least loosely, linked by a θ -rotation.

E. Fourth harmonic

The Fourier coefficient of the fourth harmonic of orientation distribution function for a rigid dumbbell suspension in large-amplitude oscillatory shear flow is given by

$$\psi'_4 = \left\{ -\frac{5(216W^3 - 201W^2 - 497W + 16)(3C^2 - 1)}{133056(W + 1)(4W + 1)(9W + 1)(9W + 25)(16W + 1)} - \frac{5(17496W^4 - 20979W^3 - 58383W^2 - 31526W + 1150)(1 - C^2)c_2}{12096(W + 1)(4W + 1)(9W + 1)(9W + 25)(16W + 1)(81W + 100)} \right\}, \quad (19)$$

and

$$\psi''_4 = \left\{ \frac{(18549162W^3 + 21819195W^2 + 7990963W - 3933950)(3C^2 - 1)}{6519744(W + 1)(4W + 1)(9W + 1)(9W + 25)(16W + 1)(81W + 100)} + \frac{(737586W^3 + 160560W^2 - 29711W - 63725)(1 - C^2)c_2}{12096(W + 1)(4W + 1)(9W + 1)(9W + 25)(16W + 1)(81W + 100)} \right\}_{\lambda\omega}. \quad (20)$$

Figures 16 (Multimedia view)–18 (Multimedia view) illustrate the orientation distribution associated with the polymer motions arising at four times the test frequency, 4ω , which are induced by the oscillatory shear deformation, and predicted by Eqs. (19) and (20), as we progress from nonlinear steady shear flow to nonlinear viscoelasticity and to linear viscoelasticity (see this progression illustrated in Figure 3). Figures 16 (Multimedia view)–18 (Multimedia view), all share the same general shape. They all represent very slight contributions to the polymer molecular motion that is dominated by the zeroth (which the peanut shapes) and the second (which imparts the tilt). These contributions, be they in the linear or the nonlinear flow regimes, take the form of three-member shish-kebabs.

Equations (11)–(20) are the main results of this work. From Figure 19 or Figure 20, we learn that for nonlinear behaviors (be they in nearly time steady shearing flow or the fully nonlinear viscoelastic regime) the orientation distribution is peanut-shaped (called lemniscoidal⁴⁰). Comparing Figures 4–18 (Multimedia view) with Figures 19–Figure 21, we learn that the lemniscoidal shape of the polymer orientation is imparted by the even harmonics, and specifically by the zeroth and second harmonics, but not by the fourth.

Examining Figure 21, we see that the overall orientation distribution hardly departs from spherical, which is the shape for a liquid at rest. In other words, only very slight departures

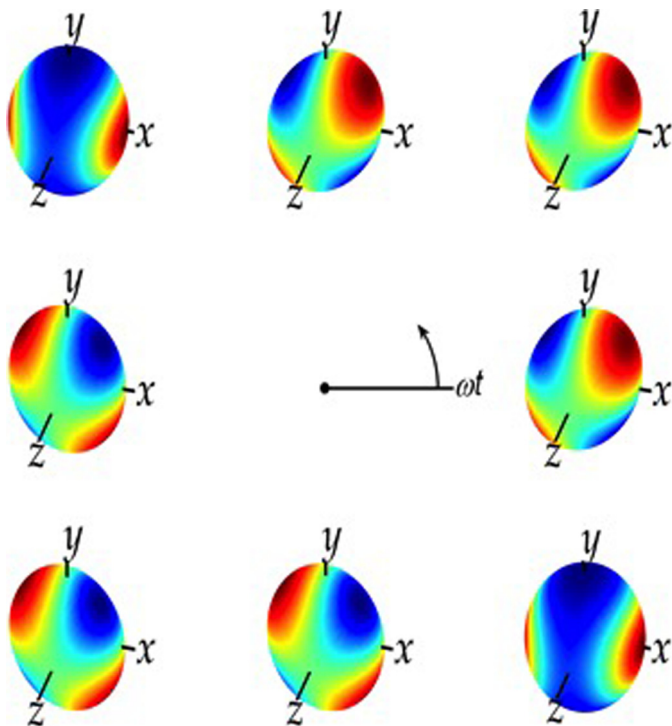


FIG. 21. Sum of first five harmonics of ψ , $\sum_{n=0}^4 [\psi'_n \cos n\omega t + \psi''_n \sin n\omega t]$ with Eqs. (11)–(20), over a complete alternant cycle of $\omega t = 0$ to $\omega t = 2\pi$, with $\lambda\omega = 1$ and $\lambda\dot{\gamma}^0 = 0.1$. Nearly linear viscoelastic regime.

from this sphericity explain the elastic behavior observed for polymeric liquids for small-amplitude oscillatory shear flow.

IV. CONCLUSION

In this paper, we have deepened our understanding of the molecular motion underlying large-amplitude oscillatory shear flow of polymeric liquids by decomposing the orientation distribution function into its first five Fourier components (the zeroth, first, second, third, and fourth harmonics). We did so for the simplest molecular model, the suspension of non-interacting rigid dumbbells in a Newtonian suspending fluid. We have used three-dimensional images to explore each harmonic of the polymer motion. Our analysis includes the three most important cases: (i) nonlinear steady shear flow, (ii) nonlinear viscoelasticity, and (iii) linear viscoelasticity.

We have learned that the polymer orientation distribution is spherical in the linear viscoelastic regime, and otherwise tilted and peanut-shaped. Further, we find that the peanut-shaping is mainly caused by the zeroth harmonic, and the tilting by the second. The first, third, and fourth harmonics of the orientation distribution make only slight contributions to the overall polymer motion.

ACKNOWLEDGMENTS

A. J. Giacomin is indebted to the Faculty of Applied Science and Engineering of Queen's University at Kingston, for its support through a Research Initiation Grant (RIG). This research was undertaken, in part, thanks to funding from the Canada Research Chairs program of the Government of Canada of the Tier 1 Canada Research Chair in Rheology.

¹A. Gemant, "Komplexe Viskosität," *Naturwissenschaften* **23**(25), 406–407 (1935).

²A. Gemant, "The conception of a complex viscosity and its application to dielectrics," *Trans. Faraday Soc.* **31**, 1582–1590 (1935).

³R. B. Bird and A. J. Giacomin, "Who conceived the complex viscosity?," *Rheol. Acta* **51**(6), 481–486 (2012).

- ⁴J. D. Ferry, *Viscoelastic Properties of Polymers*, 1st ed. (John Wiley & Sons, Inc., New York, 1961).
- ⁵J. M. Dealy, *Rheometers for Molten Plastics: A Practical Guide to Testing and Property Measurement* (Van Nostrand, New York, 1982).
- ⁶J. M. Dealy and J. Wang, *Melt Rheology and its Applications in the Plastics Industry*, 2nd ed. (Springer, Dordrecht, 2013).
- ⁷K. Weissenberg, "Rheology of hydrocarbon gels," *Proc. R. Soc. London, Ser. A* **200**(1061), 183–188 (1950).
- ⁸K. Weissenberg, in Proceedings of First International Congress on Rheology (Holland, 1948/9), pp. 1–29.
- ⁹K. Hyun, M. Wilhelm, C. O. Klein, K. S. Cho, J. G. Nam, K. H. Ahn, S. J. Lee, R. H. Ewoldt, and G. H. McKinley, "A review of nonlinear oscillatory shear tests: Analysis and application of large amplitude oscillatory shear (LAOS)," *Prog. Polym. Sci.* **36**, 1697–1753 (2011).
- ¹⁰A. J. Giacomin, T. Samurkas, and J. M. Dealy, "A novel sliding plate rheometer for molten plastics," *Polym. Eng. Sci.* **29**(8), 499–504 (1989).
- ¹¹A. J. Giacomin, "A sliding plate melt rheometer incorporating a shear stress transducer," Ph.D. thesis (Department of Chemical Engineering, McGill University, Montréal, 1987).
- ¹²A. J. Giacomin and J. M. Dealy, "A new rheometer for molten plastics," S.P.E. Tech. Papers, XXXII, in *Proceedings of 44th Annual Technical Conference, Society of Plastics Engineers*, Boston, MA (1986), pp. 711–714.
- ¹³J. E. Roberts, "The early development of the rheogoniometer," in *Karl Weissenberg: 80th Birthday Celebration Essays*, edited by J. Harris (East African Literature Bureau, Kampala, 1973), pp. 153–163.
- ¹⁴J. G. Oakley, J. A. Yosick, and A. J. Giacomin, "Molecular origins of nonlinear viscoelasticity," *Mikrochim. Acta* **130**, 1–28 (1998).
- ¹⁵A. J. Giacomin, R. B. Bird, L. M. Johnson, and A. W. Mix, "Large-amplitude oscillatory shear flow from the corotational Maxwell model," *J. Non-Newtonian Fluid Mech.* **166**(19–20), 1081–1099 (2011). Errata: after Eq. (20), Ref. 10 should be Ref. 13; in Eq. (66), "20De²" and "10De² – 50De⁴" should be "20De" and "(10De – 50De³)De" and so Figs. 15–17 of Ref. (40) below replace Figs. 5–7; on the ordinates of Figs. 5–7, $\frac{1}{2}$ should be 2; after Eq. (119), " (ζx) " should be " $\zeta(\alpha)$ "; in Eq. (147), " $n - 1$ " should be " $n = 1$ "; in Eqs. (76) and (77), Ψ' and Ψ'' should be Ψ'_1 and Ψ''_1 ; throughout, Ψ'_1 , Ψ'_1 , and Ψ''_1 should be Ψ^d_1 , Ψ'_1 , and Ψ''_1 ; in Eq. (127), "cos τ " should be " $(-\cos \tau)$ "; after Eq. (136), "Eq. (134)" should be "Eqs. (133) and (135)" and "Eq. (135)" should be "Eqs. (134) and (135)"; after Eq. (143), $|\tau_{yx}|$ should be $\dot{\gamma}$; in Eqs. (181) and (182), "1,21" should be "1,2"; in Eqs. (184) and (185), " mp " should be "1, mp "; Eq. (65) should be $We/De > \sqrt[n]{(hn + 1)}$; see also Ref. 16 below.
- ¹⁶A. J. Giacomin, R. B. Bird, L. M. Johnson, and A. W. Mix, "Corrigenda: 'Large-amplitude oscillatory shear flow from the corotational Maxwell model,'" *J. Non-Newtonian Fluid Mech.* **166**, 1081–1099 (2011), *J. Non-Newtonian Fluid Mech.* **187–188**, 1–48 (2012); see also Ref. 15 above.
- ¹⁷R. B. Bird and R. C. Armstrong, "Time-dependent flows of dilute solutions of rodlike macromolecules," *J. Chem. Phys.* **56**, 3680 (1972). Addendum: In Eq. (8), the term $-\frac{1}{432} \left[\frac{3}{49} \left(\frac{7}{3}, 0, 1; t \right) + \frac{30}{539} \left(0, \frac{7}{3}, 1; t \right) \right] P_4^2 s_2$ should be inserted just before the "+ additional terms."
- ¹⁸R. B. Bird, O. Hassager, R. C. Armstrong, and C. F. Curtiss, *Dynamics of Polymeric Liquids*, 1st ed. (Wiley, New York, 1977), Vol. 2. Erratum: In Problem 11.C.1 d., "and ϕ_2 " should be "through ϕ_4 "; On p. N-2, under L entry "Length of a rigid dumbbell connector" should be "Bead center to center length of a rigid dumbbell."
- ¹⁹F. Ding, A. J. Giacomin, R. B. Bird, and C.-B. Kweon, "Viscous dissipation with fluid inertia in oscillatory shear flow," *J. Non-Newtonian Fluid Mech.* **86**(3), 359–374 (1999).
- ²⁰J. A. Yosick, A. J. Giacomin, W. E. Stewart, and F. Ding, "Fluid inertia in large amplitude oscillatory shear," *Rheol. Acta* **37**, 365–373 (1998).
- ²¹A. J. Giacomin and J. M. Dealy, "Using large-amplitude oscillatory shear," in *Rheological Measurement*, 2nd ed., edited by A. A. Collyer and D. W. Clegg (Kluwer Academic Publishers, Dordrecht, Netherlands, 1998), Chap. 11, pp. 327–356.
- ²²A. J. Giacomin and J. M. Dealy, "Large-amplitude oscillatory shear," *Techniques in Rheological Measurement*, edited by A. A. Collyer (Chapman and Hall, London, New York, 1993), Chap. 4, pp. 99–121; Kluwer Academic Publishers, Dordrecht (1993), pp. 99–121; Erratum: Corrections to Figs 11.5–11.7 are in Ref. 21 above.
- ²³R. H. Ewoldt, "Defining nonlinear rheological material functions for oscillatory shear," *J. Rheol.* **57**, 177–195 (2013).
- ²⁴O. O. Park and G. G. Fuller, "Dynamics of rigid dumbbells in confined geometries. II. Time-dependent shear flow," *J. Non-Newton. Fluid* **18**, 111–122 (1985).
- ²⁵O. O. Park, "Dynamics of rigid and flexible polymer chains. I. Transport through confined geometries," Ph.D. thesis (Chemical Engineering, Stanford University, Stanford, CA, 1985).
- ²⁶R. B. Bird, H. R. Warner, Jr., and D. C. Evans, "Kinetic theory and rheology of dumbbell suspensions with Brownian motion," *Adv. Polym. Sci. (Fortschr. Hochpolymeren-Forschung)* **8**, 1–90 (1971).
- ²⁷R. B. Bird, C. F. Curtiss, R. C. Armstrong, and O. Hassager, *Dynamics of Polymeric Liquids*, 2nd ed. (John Wiley & Sons, Inc., New York, 1987), Vol. 2. Erratum: On p. 409 of the first printing, the $(n+m)!$ in the denominator should be $(n-m)!$; In Table 16.4-1, under L entry "length of rod" should be "bead center to center length of a rigid dumbbell." In the Figure 14.1-2 caption, "Multibead rods of length L " should be "Multibead rods of length $L+d$ ".
- ²⁸J. G. Kirkwood and R. J. Plock, "Non-Newtonian viscoelastic properties of rod-like macromolecules in solution," *J. Chem. Phys.* **24**, 665–669 (1956).
- ²⁹J. G. Kirkwood and R. J. Plock, "Non-Newtonian viscoelastic properties of rod-like macromolecules in solution," in *Macromolecules*, edited by P. L. Auer (Gordon and Breach, New York, 1967), pp. 113–121. Errata: On the left side of Eq. (1) on p. 113, ϵ should be $\dot{\epsilon}$. See also Eq. (1) of Ref. 28. In Eq. (2a), G' should be G'' , and in Eq. (2b), G'' should be G' . See Eqs. (117a) and (117b) of Ref. 32.
- ³⁰R. J. Plock, "I. non-Newtonian viscoelastic properties of rod-like macromolecules in solution. II. The Debye-Hückel, Fermi-Thomas theory of plasmas and liquid metals," Ph.D. thesis (Yale University, New Haven, CT, 1957). Errata: In Eq. (2.4a), G' should be G'' , and in Eq. (2.4b), G'' should be G' . See Eqs. (117a) and (117b) of Ref. 32.
- ³¹E. Paul, "Non-Newtonian viscoelastic properties of rodlike molecules in solution: comment on a paper by Kirkwood and Plock," *J. Chem. Phys.* **51**, 1271–1290 (1969).
- ³²E. W. Paul, "Some non-equilibrium problems for dilute solutions of macromolecules. I. The plane polygonal polymer," Ph.D. thesis (Department of Chemistry, University of Oregon, Eugene, OR, 1970).

- ³³N. A. K. Bharadwaj, "Low dimensional intrinsic material functions uniquely identify rheological constitutive models and infer material microstructure," Masters thesis (Mechanical Engineering, University of Illinois at Urbana-Champaign, IL, 2012).
- ³⁴E. W. Paul and R. M. Mazo, "Hydrodynamic properties of a plane-polygonal polymer, according to Kirkwood-Riseman theory," *J. Chem. Phys.* **51**, 1102–1107 (1969).
- ³⁵C. Y. Mou and R. M. Mazo, "Normal stress in a solution of a plane-polygonal polymer under oscillating shearing flow," *J. Chem. Phys.* **67**, 5972–5973 (1977).
- ³⁶E. Helfand and D. S. Pearson, "Calculation of the nonlinear stress of polymers in oscillatory shear fields," *J. Polym. Sci.: Polym. Phys. Ed.* **20**, 1249–1258 (1982).
- ³⁷R. B. Bird, A. J. Giacomin, A. M. Schmalzer, and C. Aumann, "Dilute rigid dumbbell suspensions in large-amplitude oscillatory shear flow: Shear stress response," *J. Chem. Phys.* **140**, 074904 (2014); Corrigenda: In Eq. (91), η' should be η'' . In caption to Fig. 3, " $\psi_1[P_2^2 s_2]$ " should be " $\cos 3\omega t$ " and " $\psi_2[P_2^0 c_0, P_2^2 c_2, \dots]$ " should be " $\sin 3\omega t$ ".
- ³⁸A. M. Schmalzer, R. B. Bird, and A. J. Giacomin, "Normal stress differences in large-amplitude oscillatory shear flow for dilute rigid dumbbell suspensions," PRG Report No. 002, QU-CHEE-PRG-TR-2014-2, Polymers Research Group, Chemical Engineering Department, Queen's University, Kingston, CANADA, 2014.
- ³⁹A. M. Schmalzer, R. B. Bird, and A. J. Giacomin, "Normal stress differences in large-amplitude oscillatory shear flow for dilute rigid dumbbell suspensions," *J. Non-Newtonian Fluid Mech.* (2014); Errata: Above Eqs. (14) and (25), "significant figures" should be "16 significant figures."
- ⁴⁰A. M. Schmalzer and A. J. Giacomin, "Orientation in large-amplitude oscillatory shear," *Macromol. Theory Simul.* **23**, 1–27 (2014).
- ⁴¹A. M. Schmalzer and A. J. Giacomin, "Orientation in large-amplitude oscillatory shear," PRG Report No. 005, QU-CHEE-PRG-TR-2014-5, Polymers Research Group, Chemical Engineering Department, Queen's University, Kingston, CANADA, 2014.
- ⁴²A. M. Schmalzer, "Large-amplitude oscillatory shear flow of rigid dumbbell suspensions," Ph.D. thesis (University of Wisconsin, Mechanical Engineering Department, Madison, WI, 2014).
- ⁴³Y. Bozorgi, "Multiscale simulation of the collective behavior of rodlike self-propelled particles in viscoelastic fluids," Ph.D. thesis (Chemical and Biological Engineering, Rensselaer Polytechnic Institute, Troy, NY, 2014).
- ⁴⁴Y. Bozorgi and P. T. Underhill, "Large-amplitude oscillatory shear rheology of dilute active suspensions," *Rheol. Acta* **53**, 899–909 (2014).
- ⁴⁵C. Saengow, A. J. Giacomin, and C. Kolitawong, "Exact analytical solution for large-amplitude oscillatory shear flow," PRG Report No. 008, QU-CHEE-PRG-TR-2014-8, Polymers Research Group, Chemical Engineering Dept., Queen's University, Kingston, 2014.